Electronic structure of random binary alloys: An augmented space formulation in reciprocal space

Kamal Krishna Saha* and Abhijit Mookerjee†
S. N. Bose National Centre for Basic Sciences, JD Block, Sector III, Salt Lake City, Kolkata 700098, India

Ove Jepsen‡
Max-Planck Institut für Festkörperforschung, Postfach 800665, D-70506 Stuttgart, Germany
(Received 17 September 2004; revised manuscript received 10 December 2004; published 30 March 2005)

We present here a reciprocal space formulation of the augmented space recursion which uses the lattice translation symmetry in the full augmented space to produce configuration-averaged quantities, such as spectral functions and complex band structures. Since the real space part is taken into account *exactly* and there is no truncation of this in the recursion, the results are more accurate than recursions in real space. We have also described the Brillouin zone integration procedure to obtain the configuration-averaged density of states. We apply the technique to the $Ni_{50}Pt_{50}$ alloy in conjunction with the tight-binding linear-muffin-tin orbital basis. These developments in the theoretical basis were necessitated by our future application to obtain optical conductivity in random systems.

DOI: 10.1103/PhysRevB.71.094207 PACS number(s): 71.23.−k

I. INTRODUCTION

The augmented space recursion (ASR) carried out in a minimal basis set representation of the tight-binding linear-muffin-tin orbital method (TB LMTO) has been proposed earlier by us[1,2] as an interesting technique for incorporation of the effects of configuration fluctuations about the mean field [the coherent potential approximation (CPA)] for random substitutionally disordered alloys. This can be achieved without the usual problems of violation of the Herglotz analytic properties[3] of the approximated configuration-averaged Green's functions for the Schrödinger equation for these random alloys. Earlier we had used this technique to look at short-ranged ordering in such systems,[4,5] as well as local lattice distortions caused by size difference between the constituents of the alloy.[6]

One of the dissatisfying features of the method, and this has to do with the recursion part, is the truncation of the continued fraction expansion of the Green's function. Truncation in the configuration space part of the problem can be handled easily. We truncate out only those configurations that occur with low probability and contribute to the tail of the continued fraction. It is on the truncation in real space that we do not have a controllable handle. Any truncation in real space means that our recursion has been carried out on a finite cluster and edge effects become important. Quantities that converge fast are integrals of the density of states multiplied by well-behaved functions of energy. We can also estimate the errors committed by truncating at a particular step.[7] However, the errors in the density of states itself cannot be controlled. This is because even a small perturbation (like truncation after a large number of recursive steps) has a profound effect on the spectrum of the Hamiltonian (see Haydock[8]). The problem of truncation has always been laid at the door of the recursion method.

Is it not possible to modify the TB LMTO ASR in such a way that the truncation is carried out only in configuration space? One way of reducing the gigantic rank of the Hamiltonian in a real-space-labeled basis is to go over to reciprocal space. In the **k**-labeled basis, for a basis involving only *s*, *p*, and *d* states, the operators in reciprocal space have rank 9. However, to do this we require lattice translational symmetry. In a random binary alloy, for instance, this is not immediately possible. However, the full augmented space, which is the direct product of the real space spanned by the site-labeled basis $\{R_i\}$ and the configuration space spanned by the configurations of the system, possesses translational as well as point group symmetries.[9] Configurations of a binary alloy can be labeled by a binary sequence of 0 and 1 (or ↑ and ↓ if Ising models appeal to you more) and uniquely described by the cardinality sequence $\{C\}$, i.e., the sequence of positions where we have a 1 or a ↓ state. We had shown earlier that in the subspace spanned by the reference states $\{\emptyset\}$, in which the configuration average is described, we have full lattice translation symmetry provided the disorder is homogeneous.[10] The same statement would be true if there is short-ranged order or local lattice distortions, provided the short-ranged order or local lattice distortions is probabilistically identical anywhere in the system. A consequence of this is that probability densities are independent of the site label and the configuration-averaged quantity

$$\sum_{R_i}\sum_{R_j} \exp\{i(\mathbf{k}\cdot R_i - \mathbf{k}'\cdot R_j)\}\langle\langle G(R_i,R_j,z)\rangle\rangle = G(\mathbf{k},z)\,\delta(\mathbf{k}-\mathbf{k}').$$

Based on this, we had proposed a TB LMTO recursion in the reciprocal augmented space.[11] The recursion, as we shall show subsequently, is entirely in configuration space for each **k** label. The truncation is also in configuration space alone and leads to calculation of the configuration-averaged spectral densities. These spectral densities are not a bunch of δ functions, as in the case of ordered systems, but the complex self-energies, in general both energy and **k** dependent, shift

the peaks as well as broaden them, leading to fuzzy, complex band structures.

Although our method allows us to carry our augmented space recursion into reciprocal space, for many physical problems we need to carry our integration over the Brilluoin zone. For instance, to obtain the density of states or optical conductivity[12]

$$\langle\langle n(E)\rangle\rangle = \int_{\mathrm{BZ}} \frac{d^3\mathbf{k}}{8\pi^3} \mathrm{Tr}\langle\langle \mathbf{A}(\mathbf{k},E)\rangle\rangle,$$

$$\langle\langle \sigma(\omega)\rangle\rangle = \int dE \int_{\mathrm{BZ}} \frac{d^3\mathbf{k}}{8\pi^3} \mathrm{Tr}[\mathbf{J}^{\mathrm{eff}}(\mathbf{k},E,\omega) \times \langle\langle \mathbf{A}(\mathbf{k},E)\rangle\rangle \mathbf{J}^{\mathrm{eff}}(\mathbf{k},E,\omega)^{\dagger} \langle\langle \mathbf{A}(\mathbf{k},E+\omega)\rangle\rangle].$$

Here $\langle\langle \mathbf{A}(\mathbf{k},E)\rangle\rangle$ is the configuration-averaged spectral density and disorder scattering renormalizes the current term in the Kubo-Greenwood formula to $\mathbf{J}^{\mathrm{eff}}(\mathbf{k},E,\omega)$.

Another contribution of this paper is to modify the tetrahedral method of Brilluoin zone integration, so that we may carry out a similar integration technique for integrands which are smoother than the highly singular spectral functions of the ordered systems. The proposed Brilluoin zone integration is closely related to that of Jepsen and Andersen[13] or Lehmann and Taut[14] for ordered systems.

II. AUGMENTED SPACE RECURSION IN *k* SPACE

The augmented space recursion based on the tight-binding linear muffin-tin orbitals method has been described thoroughly in a series of articles,[1,2,16–19] We shall introduce the salient features of the ASR which will be required by us in our subsequent discussions.

We shall start from a first-principles tight-binding linear-muffin-tin orbitals[20,21] in the most localized representation (α representation). This is necessary, because the subsequent recursion requires a sparse representation of the Hamiltonian. In this representation, the second-order alloy Hamiltonian is given by

$$\mathbf{H}^{(2)} = \mathbf{E}_{\nu} + \mathbf{h} - \mathbf{hoh},$$

where

$$\mathbf{h} = \sum_R (\mathbf{C}_R - \mathbf{E}_{\nu R})\mathcal{P}_R + \sum_R \sum_{R'} \mathbf{\Delta}_R^{1/2} \mathbf{S}_{RR'} \mathbf{\Delta}_{R'}^{1/2} \mathcal{T}_{RR'},$$

$$\mathbf{o} = \sum_R \mathbf{o}_R \mathcal{P}_R. \tag{1}$$

$\mathbf{C}_R, \mathbf{E}_{\nu R}, \mathbf{\Delta}_R$, and $\mathbf{o}_R$ are diagonal matrices in angular momentum space:

$$\mathbf{C}_R = C_{RL}\delta_{LL'}, \quad \mathbf{E}_{\nu R} = E_{\nu RL}\delta_{LL'},$$

$$\mathbf{\Delta}_R = \Delta_{RL}\delta_{LL'}, \quad \mathbf{o}_R = o_{RL}\delta_{LL'},$$

and $\mathbf{S}_{RR'}$ is a matrix of rank $L_{\max}$. $\mathcal{P}_R = |R\rangle\langle R|$ and $\mathcal{T}_{RR'} = |R\rangle\langle R'|$ are projection and transfer operators in the Hilbert space $\mathcal{H}$ spanned by the tight-binding basis $\{|R\rangle\}$. Here, R refers to the position of atoms in the solid and L is a composite label $\{\ell, m, m_s\}$ for the angular momentum quantum numbers. $\mathbf{C}$, $\mathbf{\Delta}$, and $\mathbf{o}$ are potential parameters of the TB LMTO method; $\mathbf{o}^{-1}$ has dimension of energy and the $\mathbf{E}_{\nu}$'s are the reference energies about which the muffin-tin orbitals are linearized.

For a disordered binary alloy we may write

$$C_{RL} = C_L^A n_R + C_L^B (1 - n_R),$$

$$\Delta_{RL}^{1/2} = (\Delta_L^A)^{1/2} n_R + (\Delta_L^B)^{1/2} (1 - n_R),$$

$$o_{RL} = o_L^A n_R + o_L^B (1 - n_R). \tag{2}$$

Here $\{n_R\}$ are the random site-occupation variables which take values 1 and 0 depending upon whether the muffin-tin labeled by R is occupied by an A or B type of atom. The atom sitting at $\{R\}$ can be of either type $A(n_R=1)$ with probability x or $B(n_R=0)$ with probability y. The augmented space formalism (ASF) now introduces the space of configurations of the set of binary random variables $\{n_R\}:\Phi$.

In the absence of short-ranged order, each random variable n_R has associated with it an operator $\mathbf{M}_R$ whose spectral density is its probability density:

$$p(n_R) = x\delta(n_R - 1) + y\delta(n_R) = -\frac{1}{\pi} \lim_{\delta \to 0} \mathrm{Im}\langle\uparrow_R|[(n_R + i\delta)\mathbf{I} - \mathbf{M}_R]^{-1}|\uparrow_R\rangle, \tag{3}$$

where $\mathbf{M}_R$ is an operator whose eigenvalues 1, 0 correspond to the observed values of n_R and whose corresponding eigenvectors $\{|1_R\rangle, |0_R\rangle\}$ span a configuration space ϕ_R of rank 2. We may change the basis to $\{|\uparrow_R\rangle, |\downarrow_R\rangle\}$ (see Appendix A) and in this new basis the operator $\mathbf{M}_R$ is:

$$n_R \to \mathbf{M}_R = x\mathcal{P}_R^{\uparrow} + y\mathcal{P}_R^{\downarrow} + \sqrt{xy}(\mathcal{T}_R^{\uparrow\downarrow} + \mathcal{T}_R^{\downarrow\uparrow}). \tag{4}$$

Two new vectors span the space ϕ_R. The full configuration space $\Phi = \Pi_R^{\otimes} \phi_R$ is then spanned by vectors of the form $|\uparrow\uparrow\downarrow\uparrow\downarrow\cdots\rangle$. These configurations may be labeled by the sequence of sites $\{\mathcal{C}\}$ at which we have a $\downarrow$. For example, for the state just quoted $\{\mathcal{C}\} = |\{3,5,\ldots\}\rangle$. This sequence is called the *cardinality sequence*. If we define the configuration $|\uparrow\uparrow\cdots\uparrow\cdots\rangle$ as the *reference* configuration, then the cardinality sequence of the reference configuration is the null sequence $\{\emptyset\}$.

The augmented space theorem[16] states that

$$\langle\langle A(\{n_R\})\rangle\rangle = \langle\{\emptyset\}|\tilde{\mathbf{A}}|\{\emptyset\}\rangle, \tag{5}$$

where

$$\tilde{\mathbf{A}}(\{\mathbf{M}_R\}) = \int \cdots \int A(\{\lambda_R\}) \prod d\mathbf{P}(\lambda_R).$$

$\mathbf{P}(\lambda_R)$ is the spectral density of the self-adjoint operator $\mathbf{M}_R$.

Applying (5) to the Green's function we get

$$\langle\langle \mathbf{G}(\mathbf{k},z)\rangle\rangle = \langle \mathbf{k}\otimes\{\emptyset\}|(z\tilde{\mathbf{I}}-\tilde{\mathbf{H}}^{(2)})^{-1}|\mathbf{k}\otimes\{\emptyset\}\rangle, \quad (6)$$

where $\mathbf{G}$ and $\mathbf{H}^{(2)}$ are operators which are matrices in angular momentum space, and the augmented $\mathbf{k}$ space basis $|\mathbf{k},L\otimes\{\emptyset\}\rangle$ has the form

$$(1/\sqrt{N})\sum_R \exp(-i\mathbf{k}\cdot R)|R,L\otimes\{\emptyset\}\rangle.$$

The augmented space Hamiltonian $\tilde{\mathbf{H}}^{(2)}$ is constructed from the TB LMTO Hamiltonian $\mathbf{H}^{(2)}$ by replacing each random variable n_R by operators $\mathbf{M}_R$. It is an operator in the augmented space $\Psi=\mathcal{H}\otimes\Phi$. The ASF maps a disordered Hamiltonian described in a Hilbert space $\mathcal{H}$ onto an ordered Hamiltonian in an enlarged space Ψ, where the space Ψ is constructed as the outer product of the space $\mathcal{H}$ and configuration space Φ of the random variables of the disordered Hamiltonian. The configuration space Φ is of rank 2^N if there are N muffin-tin spheres in the system. Another way of looking at $\tilde{\mathbf{H}}^{(2)}$ is to note that it is the *collection* of all possible Hamiltonians for all possible configurations of the system.

The resolvent of the Hamiltonian can be expressed in the following way:

$$\begin{aligned}(z\mathbf{I}-\mathbf{H}^{(2)})^{-1} &= (z\mathbf{I}-\mathbf{C}-\boldsymbol{\Delta}^{1/2}\mathbf{S}\boldsymbol{\Delta}^{1/2}+\mathbf{hoh})^{-1}\\ &= \boldsymbol{\Delta}^{-1/2}\left[\frac{z\mathbf{I}-\mathbf{C}}{\boldsymbol{\Delta}}-\mathbf{S}+\left(\frac{\mathbf{C}-\mathbf{E}_\nu}{\boldsymbol{\Delta}}+\mathbf{S}\right)(\boldsymbol{\Delta}^{1/2}\mathbf{o}\boldsymbol{\Delta}^{1/2})\right.\\ &\quad\left.\times\left(\frac{\mathbf{C}-\mathbf{E}_\nu}{\boldsymbol{\Delta}}+\mathbf{S}\right)\right]^{-1}\boldsymbol{\Delta}^{-1/2}.\end{aligned}$$

Expressions in bold are matrices in angular momentum space and all others except $\mathbf{S}$, $\mathbf{H}^{(2)}$, and $\mathbf{G}$ are diagonal matrices.

In the above expression, since

$$\begin{aligned}\tilde{\boldsymbol{\Delta}}^{-1/2} = \sum_R \{&\mathbf{A}(\boldsymbol{\Delta}^{-1/2})\mathcal{P}_R\otimes\mathcal{I}+\mathbf{B}(\boldsymbol{\Delta}^{-1/2})\mathcal{P}_R\otimes\mathcal{P}_R^{\downarrow}\\ &+\mathbf{F}(\boldsymbol{\Delta}^{-1/2})\mathcal{P}_R\otimes(\mathcal{T}_R^{\uparrow\downarrow}+\mathcal{T}_R^{\downarrow\uparrow})\},\end{aligned}$$

where for any diagonal (in angular momentum space) operator $\mathbf{V}$

$$\mathbf{A}(\mathbf{V}) = A(V_L)\delta_{LL'}, \quad A(V_L) = xV_L^A + yV_L^B,$$

$$\mathbf{B}(\mathbf{V}) = B(V_L)\delta_{LL'}, \quad B(V_L) = (y-x)(V_L^A - V_L^B),$$

$$\mathbf{F}(\mathbf{V}) = F(V_L)\delta_{LL'}, \quad F(V_L) = \sqrt{xy}(V_L^A - V_L^B),$$

we get

$$\tilde{\boldsymbol{\Delta}}^{-1/2}|\mathbf{k}\otimes\{\emptyset\}\rangle = \mathbf{A}(\boldsymbol{\Delta}^{-1/2})|\mathbf{k}\otimes\{\emptyset\}\rangle + \mathbf{F}(\boldsymbol{\Delta}^{-1/2})|\mathbf{k}\otimes\{R\}\rangle = |1\}.$$

The ket $|1\}$ is not normalized and we define the normalized ket as $|1\rangle=[\mathbf{A}(\boldsymbol{\Delta}^{-1})]^{-1/2}|1\}$. Then we may rewrite (6) as

$$\langle\langle \mathbf{G}(\mathbf{k},z)\rangle\rangle = \langle 1|[z\tilde{\mathbf{I}}-\tilde{\mathbf{A}}+\tilde{\mathbf{B}}+\tilde{\mathbf{F}}-\tilde{\mathbf{S}}+(\tilde{\mathbf{J}}+\tilde{\mathbf{S}})\tilde{\mathbf{o}}(\tilde{\mathbf{J}}+\tilde{\mathbf{S}})]^{-1}|1\rangle,$$

where

$$\tilde{\mathbf{A}} = \sum_R \{\mathbf{A}(\mathbf{C}\boldsymbol{\Delta}^{-1})/\mathbf{A}(\boldsymbol{\Delta}^{-1})\}\mathcal{P}_R\otimes\mathcal{I},$$

$$\tilde{\mathbf{B}} = \sum_R \{\mathbf{B}[(z\mathbf{I}-\mathbf{C})\boldsymbol{\Delta}^{-1}]/\mathbf{A}(\boldsymbol{\Delta}^{-1})\}\mathcal{P}_R\otimes\mathcal{P}_R^{\downarrow},$$

$$\tilde{\mathbf{F}} = \sum_R \{\mathbf{F}[(z\mathbf{I}-\mathbf{C})\boldsymbol{\Delta}^{-1}]/\mathbf{A}(\boldsymbol{\Delta}^{-1})\}\mathcal{P}_R\otimes\{\mathcal{T}_R^{\uparrow\downarrow}+\mathcal{T}_R^{\downarrow\uparrow}\}, \quad (7)$$

$\tilde{\mathbf{J}}=\tilde{\mathbf{J}}_A+\tilde{\mathbf{J}}_B+\tilde{\mathbf{J}}_F$, and $\tilde{\mathbf{o}}=\tilde{\mathbf{o}}_A+\tilde{\mathbf{o}}_B+\tilde{\mathbf{o}}_F$, where

$$\tilde{\mathbf{J}}_\mathbf{A} = \sum_R \{\mathbf{A}[(\mathbf{C}-\mathbf{E}_\nu)\boldsymbol{\Delta}^{-1}]/\mathbf{A}(\boldsymbol{\Delta}^{-1})\}\mathcal{P}_R\otimes\mathcal{I},$$

$$\tilde{\mathbf{J}}_\mathbf{B} = \sum_R \{\mathbf{B}[(\mathbf{C}-\mathbf{E}_\nu)\boldsymbol{\Delta}^{-1}]/\mathbf{A}(\boldsymbol{\Delta}^{-1})\}\mathcal{P}_R\otimes\mathcal{P}_R^{\downarrow},$$

$$\tilde{\mathbf{J}}_\mathbf{F} = \sum_R \{F[(\mathbf{C}-\mathbf{E}_\nu)\boldsymbol{\Delta}^{-1}]/\mathbf{A}(\boldsymbol{\Delta}^{-1})\}\mathcal{P}_R\otimes\{\mathcal{T}_R^{\uparrow\downarrow}+\mathcal{T}_R^{\downarrow\uparrow}\},$$

$$\tilde{\mathbf{o}}_\mathbf{A} = \sum_R \{\mathbf{A}(\mathbf{o}\boldsymbol{\Delta})\mathbf{A}(\boldsymbol{\Delta}^{-1})\}\mathcal{P}_R\otimes\mathcal{I},$$

$$\tilde{\mathbf{o}}_\mathbf{B} = \sum_R \{\mathbf{B}(\mathbf{o}\boldsymbol{\Delta})\mathbf{A}(\boldsymbol{\Delta}^{-1})\}\mathcal{P}_R\otimes\mathcal{P}_R^{\downarrow},$$

$$\tilde{\mathbf{o}}_\mathbf{F} = \sum_R \{\mathbf{F}(\mathbf{o}\boldsymbol{\Delta})\mathbf{A}(\boldsymbol{\Delta}^{-1})\}\mathcal{P}_R\otimes\{\mathcal{T}_R^{\uparrow\downarrow}+\mathcal{T}_R^{\downarrow\uparrow}\}. \quad (8)$$

In case there is no off-diagonal disorder due to local lattice distortion because of size mismatch,

$$\tilde{\mathbf{S}} = \sum_R\sum_{R'} \mathbf{A}(\boldsymbol{\Delta}_R^{-1})^{-1/2}\mathbf{S}_{RR'}\mathbf{A}(\boldsymbol{\Delta}_{R'}^{-1})^{-1/2}\mathcal{T}_{RR'}\otimes\mathcal{I}.$$

This equation is now exactly in the form in which the recursion method may be applied. At this point we note that the above expression for the averaged $G_{LL}(\mathbf{k},z)$ is exact.

The recursion method addresses inversions of infinite matrices.[8] Once a sparse representation of an operator in Hilbert space, $\tilde{\mathbf{H}}^{(2)}$, is known in a countable basis, the recursion method obtains an alternative basis in which the operator becomes tridiagonal. This basis and the representations of the operator in it are found recursively through a three-term recurrence relation

$$|u_{n+1}\} = \tilde{\mathbf{H}}^{(2)}|u_n\} - \alpha_n(\mathbf{k})|u_n\} - \beta_n^2(\mathbf{k})|u_{n-1}\} \quad (9)$$

with the initial choice $|u_1\}=|RL\rangle\otimes|1\rangle$ and $\beta_1^2=1$. The recursion coefficients α_n and β_n are real and are obtained by imposing the orthonormalizability condition of the new basis set as

$$\alpha_n(\mathbf{k}) = \frac{\{n|\tilde{\mathbf{H}}^{(2)}|n\}}{\{n|n\}}, \quad \beta_{n-1}^2(\mathbf{k}) = \frac{\{n-1|\tilde{\mathbf{H}}^{(2)}|n\}}{\{n|n\}},$$

$$\text{and also} \quad \{m|\tilde{\mathbf{H}}^{(2)}|n\} = 0 \text{ for } m\neq n, n\pm 1.$$

To obtain the spectral function we first write the configuration averaged L-projected Green's functions as continued fractions:

$$\langle\langle G_{LL}(\mathbf{k},z)\rangle\rangle = \cfrac{\beta_{1L}^2}{z-\alpha_{1L}(\mathbf{k})-\cfrac{\beta_{2L}^2(\mathbf{k})}{z-\alpha_{2L}(\mathbf{k})-\cfrac{\beta_{3L}^2(\mathbf{k})}{\ddots \cfrac{}{z-\alpha_{NL}(\mathbf{k})-\mathbf{\Gamma}_L(\mathbf{k},z)}}}},$$

where $\mathbf{\Gamma}_L(\mathbf{k},z)$ is the asymptotic part of the continued fraction. The approximation involved has to do with the termination of this continued fraction. The coefficients are calculated exactly up to a finite number of steps $\{\alpha_n,\beta_n\}$ for $n<N$ and the asymptotic part of the continued fraction is obtained from the initial set of coefficients using the idea of the Beer and Pettifor terminator.[22] Haydock and co-workers[23] have carried out extensive studies of the errors involved and precise estimates are available in the literature. Haydock[24] has shown that if we carry out recursion exactly up to N steps, the resulting continued fraction maintains the first $2N$ moments of the exact result.

It is important to note that the operators $\tilde{\mathbf{A}},\tilde{\mathbf{B}},\tilde{\mathbf{F}}$ are all projection operators in real space (i.e., unit operators in $\mathbf{k}$ space) and acts on an augmented space basis only to change the configuration part (i.e., the cardinality sequence $\{\mathcal{C}\}$),

$$\widetilde{\mathbf{A}}\|\{\mathcal{C}\}\rangle = A_1\|\{\mathcal{C}\}\rangle,$$

$$\widetilde{\mathbf{B}}\|\{\mathcal{C}\}\rangle = A_2\|\{\mathcal{C}\}\rangle\delta(R\in\{\mathcal{C}\}),$$

$$\widetilde{\mathbf{F}}\|\{\mathcal{C}\}\rangle = A_3\|\{\mathcal{C}\pm R\}\rangle.$$

The coefficients A_1–A_3 can be expressed from Eq. (7). Similar expressions hold for the operators in Eq. (8). The remaining operator $\tilde{\mathbf{S}}$ is diagonal in $\mathbf{k}$ space and acts on an augmented space only to change the configuration part:

$$\widetilde{\mathbf{S}}\|\{\mathcal{C}\}\rangle = \sum_{\chi}\exp(-\imath\mathbf{k}\cdot\chi)\|\{\mathcal{C}-\chi\}\rangle.$$

Here the χ's are the near-neighbor vectors. The operation of the effective Hamiltonian is thus entirely in the configuration space and the calculation does not involve the space $\mathcal{H}$ at all. This is an enormous simplification over the standard augmented space recursion described earlier,[1,2,18,19] where the entire reduced real space part as well as the configuration part was involved in the recursion process. Earlier we had to resort to symmetry reduction of this enormous space in order to make the recursion tractable. Here the rank of only the configuration space is much smaller and we may further reduce it by using the local symmetries of the configuration space, as described in our earlier Letter.[1] However, this advantage is offset by the fact that the effective Hamiltonian is energy dependent. This means that to obtain the Green functions we have to carry out the recursion for each energy point. This process is simplified by carrying out recursion over a suitably chosen set of *seed energies* and interpolating the values of the coefficients across the band.

III. SPECTRAL DENSITY AND BAND ENERGY

The self-energy which arises because of scattering by the random potential fluctuations is of the form

$$\Sigma_L(\mathbf{k},z) = \cfrac{\beta_{2L}^2(\mathbf{k})}{z-\alpha_{2L}(\mathbf{k})-\cfrac{\beta_{3L}^2(\mathbf{k})}{\ddots \cfrac{}{z-\alpha_{NL}(\mathbf{k})-\mathbf{\Gamma}_L(\mathbf{k},z)}}}.$$

So the continued fraction can be written in the form $1/[z-\tilde{E}_L(\mathbf{k})-\Sigma_L(\mathbf{k},E)]$, where $\tilde{E}_L(\mathbf{k})=\alpha_{1L}(\mathbf{k})$.

The average spectral function $\langle\langle A_{\mathbf{k}}(E)\rangle\rangle$ is related to the averaged Green's function in reciprocal space as

$$\langle\langle A_{\mathbf{k}}(E)\rangle\rangle = \sum_L \langle\langle A_{\mathbf{k}L}(E)\rangle\rangle,$$

where

$$\langle\langle A_{\mathbf{k}L}(E)\rangle\rangle = -\frac{1}{\pi}\lim_{\delta\to 0+}\{\mathrm{Im}\langle\langle G_{LL}(\mathbf{k},E-i\delta)\rangle\rangle\}.$$

To obtain the complex bands for the alloy we fix a value for $\mathbf{k}$ and solve for

$$z-\tilde{E}_L(\mathbf{k})-\Sigma_L(\mathbf{k},E)=0.$$

The real part of the roots will give the position of the bands, while the imaginary part of the roots will be proportional to the lifetime. Since the alloy is random, the bands always have finite lifetimes and are fuzzy.

IV. INTEGRATION IN k SPACE

To obtain the density of states we need to integrate over the Brillouin zone,

$$\langle\langle n(E)\rangle\rangle = \sum_L \int_{\mathrm{BZ}} \frac{d^3\mathbf{k}}{8\pi^3}\langle\langle A_{\mathbf{k}L}(E)\rangle\rangle. \tag{10}$$

For ordered systems the spectral function consists of δ functions: $A_{\mathbf{k}}^0(E)=\Sigma_j A_j\delta(E-E_j(\mathbf{k}))$, with j labeling a particular energy band. The integrand being highly singular, the integral (10) has to be calculated carefully. Jepsen and Andersen[13] and Lehmann and Taut[14] proposed an accurate technique, the tetrahedron method, for obtaining such integrals accurately. We may also mention here an earlier work[15] which extended the tetrahedron method to the complex energy plane. However, the authors did not extend it to disordered systems with an energy and wave-vector-dependent self-energy. In this section we shall discuss an extension of that method for application to disordered systems.

In the presence of disorder the spectral function is smoother and we may rewrite it in terms of the real and imaginary parts of the disorder-induced self-energy:

$$\langle\langle A_{\mathbf{k}L}(E)\rangle\rangle = \frac{-\Sigma_L^I(\mathbf{k},E)/\pi}{[E-\tilde{E}_L(\mathbf{k})-\Sigma_L^R(\mathbf{k},E)]^2+\Sigma_L^I(\mathbf{k},E)^2}. \tag{11}$$

Such a function is peaked around the zeros of $E-\tilde{E}_L(\mathbf{k})-\Sigma_L^R(\mathbf{k},E)$ and the $\Sigma_L^I(\mathbf{k},E)$ provides the width of the peaks.

The spectral function behaves roughly as *Lorentzian* in the vicinity of its peaks. We may reduce the above expression to one amenable to the tetrahedron integration form by the following trick:

$$= \int dE' \frac{-\Sigma_L^I(\mathbf{k},E)/\pi}{[E-E'-\Sigma_L^R(\mathbf{k},E)]^2+\Sigma_L^I(\mathbf{k},E)^2}\delta(E'-\tilde{E}_L(\mathbf{k}))$$

$$= \int dE' \mathcal{W}_{\mathbf{k}L}(E,E')\delta(E'-\tilde{E}_L(\mathbf{k}))$$

where $\mathcal{W}_{\mathbf{k}L}$ is defined as a *weight function*. Now integrating above over the Brillouin zone, we may get the configuration-averaged density of states (DOS)

$$\langle\langle n(E)\rangle\rangle = \sum_L \int_{\mathrm{BZ}} \frac{d^3\mathbf{k}}{8\pi^3}\langle\langle A_{\mathbf{k}L}(E)\rangle\rangle$$

$$= \sum_L \int dE' \int_{\mathrm{BZ}} \frac{d^3\mathbf{k}}{8\pi^3}\mathcal{W}_{\mathbf{k}L}(E,E')\delta(E'-\tilde{E}_L(\mathbf{k})).$$

At this stage, in order to simplify notation we shall drop the L index from all L-dependent factors and understood that the eventual result is summed over all L. In order to perform the above integration over the BZ, we have generalized the tetrahedron method developed by Jepsen and Andersen[13] and Lehmann and Taut[14] to include the weight function $\mathcal{W}_k(E,E')$. We have followed the idea of MacDonald *et al.*[25] In this generalization the energies as well as the weight functions are linearly interpolated throughout the vertices of small tetrahedrons. We label the energies at the vertices of the ith tetrahedron $\tilde{E}_1^i$, $\tilde{E}_2^i$, $\tilde{E}_3^i$, and $\tilde{E}_4^i$, where the indices correspond to increasing magnitude of the energy, i.e., $\tilde{E}_1^i \geqslant \tilde{E}_2^i \geqslant \tilde{E}_3^i \geqslant \tilde{E}_4^i$, and the corner values of the weight function are $\mathcal{W}_1^i$, $\mathcal{W}_2^i$, $\mathcal{W}_3^i$, and $\mathcal{W}_4^i$. Then the averaged DOS may be written as

$$\langle\langle n(E)\rangle\rangle = V_{\mathrm{MZ}} \int dE' \sum_{i=1}^{N} C^i \sum_{k=1}^{4} I_k^i \mathcal{W}_k^i, \tag{12}$$

where $I_k^i = I_k(E,E',\tilde{E}_1^i,\tilde{E}_2^i,\tilde{E}_3^i,\tilde{E}_4^i)$, N is the number of tetrahedral microzones, and V_{MZ} is the microzone volume, and also for $\tilde{E}_1^i < E' \leqslant \tilde{E}_2^i$,

$$C^i = 3F_{21}F_{31}F_{41}/(E'-\tilde{E}_1),$$

$$I_1^i = (F_{12}+F_{13}+F_{14})/3,$$

$$I_k^i = F_{k1}/3, \quad k=2,3,4;$$

for $\tilde{E}_2^i < E' \leqslant \tilde{E}_3^i$,

$$C^i = 3(F_{23}F_{31}+F_{32}F_{24})/E_{41},$$

$$I_1^i = F_{14}/3 + F_{13}F_{31}F_{23}/C^iE_{41},$$

$$I_2^i = F_{23}/3 + F_{24}^2F_{32}/C^iE_{41},$$

$$I_3^i = F_{32}/3 + F_{31}^2F_{23}/C^iE_{41},$$

$$I_4^i = F_{41}/3 + F_{42}F_{24}F_{32}/C^iE_{41};$$

for $\tilde{E}_3^i < E' \leqslant \tilde{E}_4^i$,

$$C^i = 3F_{14}F_{24}F_{34}/(\tilde{E}_4-E'),$$

$$I_k^i = F_{k4}/3, \quad k=1,2,3,$$

$$I_4^i = (F_{41}+F_{42}+F_{43})/3,$$

where $E_{mn}=\tilde{E}_m-\tilde{E}_n$ and $F_{mn}=(E'-\tilde{E}_n)/E_{mn}$. Also $\langle\langle n(E)\rangle\rangle$ is zero for $E' \leqslant \tilde{E}_1^i$ or $E' \geqslant \tilde{E}_4^i$.

The optical conductivity expression given in Sec. I can also be reduced to a form suitable for the generalized **k**-space integration method described above. We may write

$$\langle\langle\sigma(\omega)\rangle\rangle = \mathrm{Tr}\int dE \int dE' \int_{\mathrm{BZ}} \frac{d^3\mathbf{k}}{8\pi^3}\mathbf{J}^{\mathrm{eff}}(\mathbf{k},E,\omega)\frac{-\boldsymbol{\Sigma}^I(\mathbf{k},E)/\pi}{[E-E'-\boldsymbol{\Sigma}^R(\mathbf{k},E)]^2+\boldsymbol{\Sigma}^I(\mathbf{k},E)^2}\times\cdots$$

$$\times\,\mathbf{J}^{\mathrm{eff}}(\mathbf{k},E,\omega)^\dagger\frac{-\boldsymbol{\Sigma}^I(\mathbf{k},E)/\pi}{[E+\omega-E'-\boldsymbol{\Sigma}^R(\mathbf{k},E+\omega)]^2+\boldsymbol{\Sigma}^I(\mathbf{k},E+\omega)^2}\delta(E'-\tilde{E}_L(\mathbf{k}))$$

$$= \mathrm{Tr}\int dE \int dE' \int_{\mathrm{BZ}} \frac{d^3\mathbf{k}}{8\pi^3}\mathbf{W}_{\mathbf{k}}(E,E',\omega)\delta(E'-\tilde{E}_L(\mathbf{k})) = V_{\mathrm{MZ}}\mathrm{Tr}\int dE \int dE' \sum_{i=1}^{N} C^i \sum_{k=1}^{4} I_k^i \mathbf{W}_k^i. \tag{13}$$

This is a form similar to Eq. (12), with **W** being the corresponding weight function and $\mathbf{W}^i$ the values of this weight function at the four corners of the ith tetrahedron. The integration is carried out in a very similar fashion.

V. COMPUTATIONAL DETAILS AND RESULTS

For ordered faces the calculations have been performed in the basis of linear muffin-tin orbitals in the atomic sphere approximation including combined corrections. The scalar-

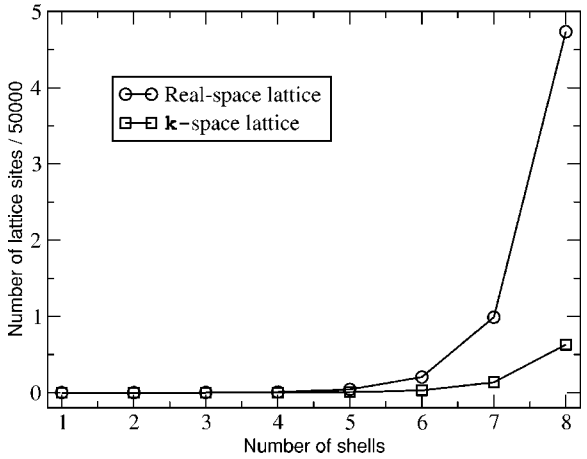

FIG. 1. Showing how the number of lattice sites increases with increasing number of shells in the real space and reciprocal space maps.

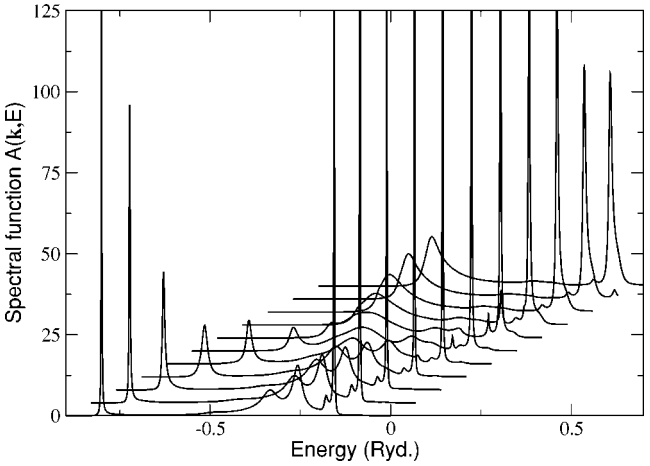

FIG. 3. The spectral function of $Ni_{50}Pt_{50}$ alloy plotted as a function of energy at several **k** points along the Γ-*X* direction.

relativistic calculations in this case are carried out for equal atomic spheres. The **k** space integration was carried out with a $16\times16\times16$ mesh resulting in 145 **k** points for cubic primitive structure in the irreducible part of the Brillouin zone.

In Fig. 1 shows how the size of the augmented space map (in both the **k** and the real space representation) increases as we increase the number of nearest-neighbor shells from a starting site. We note that the reciprocal space map at a particular recursion step is much smaller than the real augmented space map. This is because in the reciprocal augmented space we generate only the different configurations. The full real space lattice map has been collapsed using lattice translational symmetry in full augmented space.

We have first carried out calculations on a simple model of a disordered binary alloy system described by an *s*-state tight-binding Hamiltonian with nearest-neighbor hopping integrals only. In Fig. 2 we compare the results obtained using reciprocal and real space formulation of ASR. The **k** space integration has been performed in two ways. The brute force method, where we replace the integral by a sum with appropriate weights at different **k** points, generates some unusual oscillations particularly in the lower part of the band. However, the tetrahedron method gives smoother results which are in good agreement with the real space calculations as well.

We now go over to calculations for the disordered $Ni_{50}Pt_{50}$ alloy. We have used the minimal basis set of the TB LMTO with nine orbitals per atom (*s*, *p* and *d*) to set up our Hamiltonian. In Fig. 3 we present the results for the spectral functions for $Ni_{50}Pt_{50}$ alloy along the Γ-*X* direction. We have chosen 11 equidistant **k** points between the Γ and *X* points and show the spectral function at those points. These spectral functions show good agreement with the same results obtained from Korringa-Kohn-Rostocker (KKR) CPA calculations.[26] It may be seen that the width of the spectral function varies considerably as a function of **k** and *E*. There are some simple trends concerning this behavior. The sharp peaks on the lower band edge near the Γ point appear as the *s*-like band. As we go from Γ toward the *X* point the *s* band hybridizes with the *p* band and the peak becomes wider. The structures on the upper band edges are mostly due to the

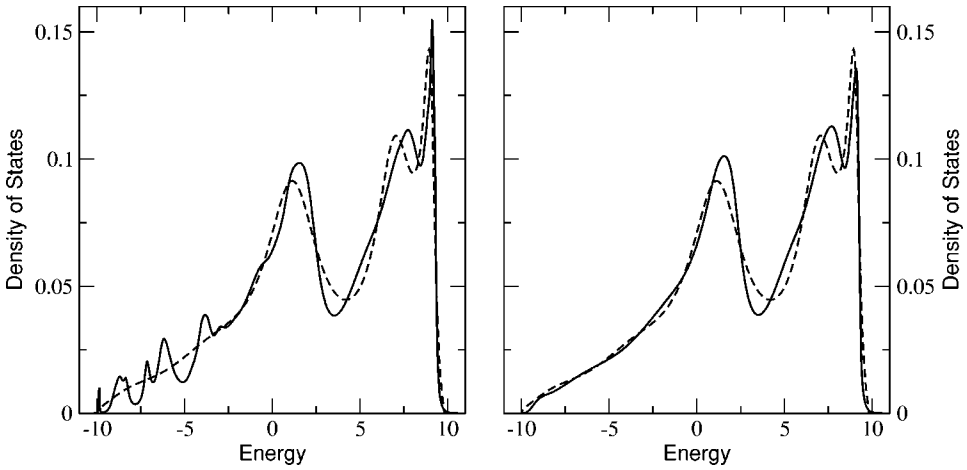

FIG. 2. Comparison of the average (50-50) density of states for a model fcc alloy calculated using the **k** space formulation of ASR (solid curve) and using real space formulation of ASR (dotted curve). **k** space integration has been performed in two ways: (a) using the tetrahedron method (TM) (right solid curve) and (b) multiplying spectral function $A_k(E)$ by the **k**-point weight and then summing up over **k** (left solid curve). In both figures we note that the oscillations shown by the brute force technique are smoothed by the TM.

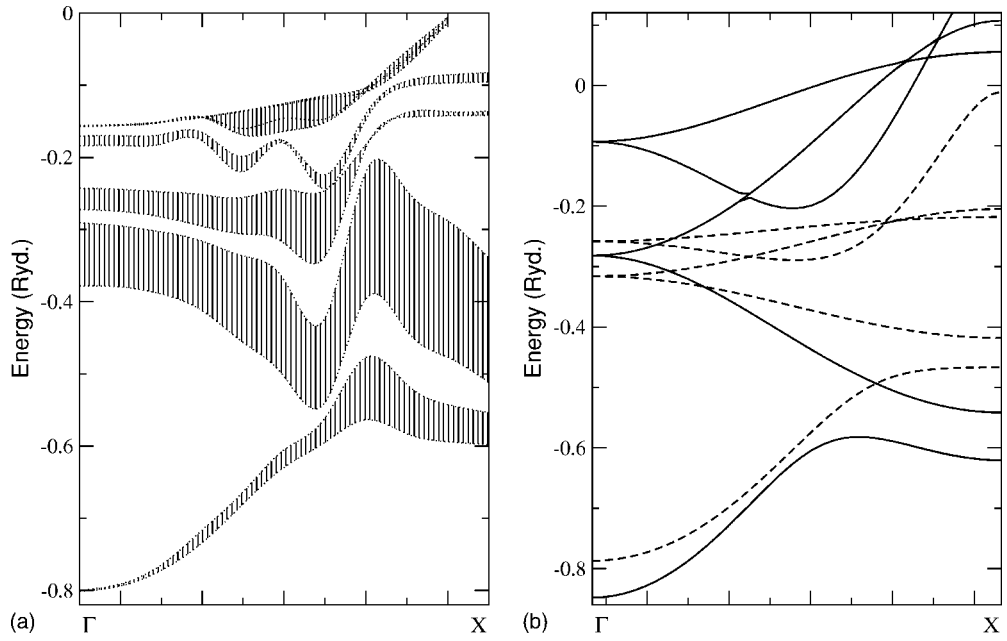

FIG. 4. (Right) Ni (dashed lines) and Pt (bold lines) energy bands on a lattice appropriate to the $Ni_{50}Pt_{50}$ alloy, in the Γ-*X* direction. Average lattice parameter $a_0=7.127$ a.u. was fixed after minimizing the energy. (Left) The fuzzy band of the disordered $Ni_{50}Pt_{50}$ system plotted along the same direction.

overlap of the *d* states of Ni and Pt. The disorder effects on these *d*-dominated states are strong and there is significant broadening.

In Fig. 4 we present the complex fuzzy bands of the disordered alloy. The disorder smearing is maximum in the overlapping *d* bands of the constituents, and is negligible in the *s*-like part. This is also apparent in the spectral functions shown earlier. The sharp *s*-like peaks flank wide *d*-like structures in Fig. 3.

Finally using our modified tetrahedron method we have calculated the density of states of ordered and homogeneous disordered NiPt alloys from the spectral function. Side by side we have also carried out the same calculation in real augmented space. In Fig. 5 we show the ℓ-projected density of states for the $Ni_{50}Pt_{50}$ alloy. We compare the **k** space results with those found from real space recursion. The main improvement occurs in the e_g and t_{2g} *d* bands. In particular, the sharp feature straddling the Fermi energy is better repro-

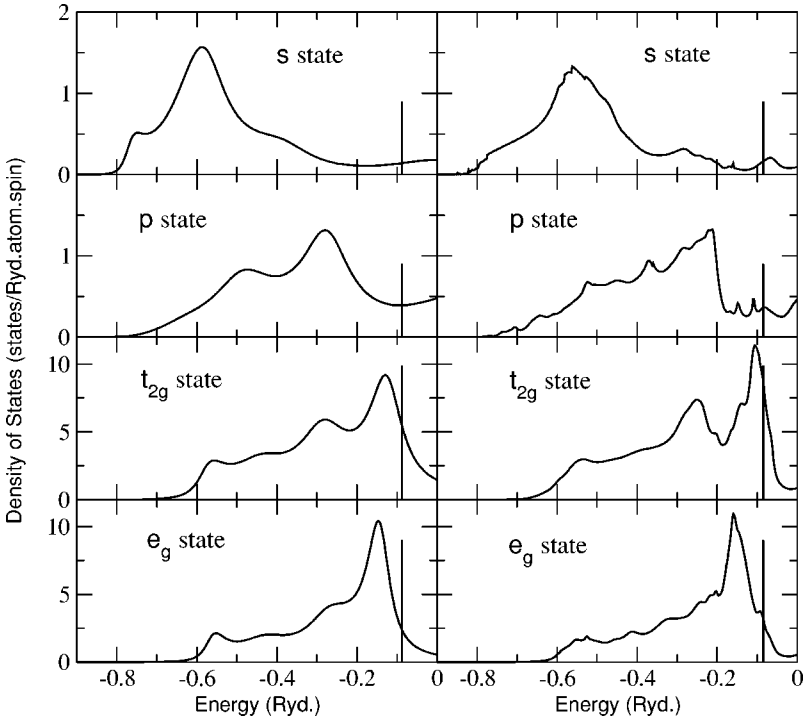

FIG. 5. Comparison of the partial density of states of $Ni_{50}Pt_{50}$ alloy calculated using augmented space recursion in (a) real space formulation (left panel) and (b) **k** space formulation (right panel).

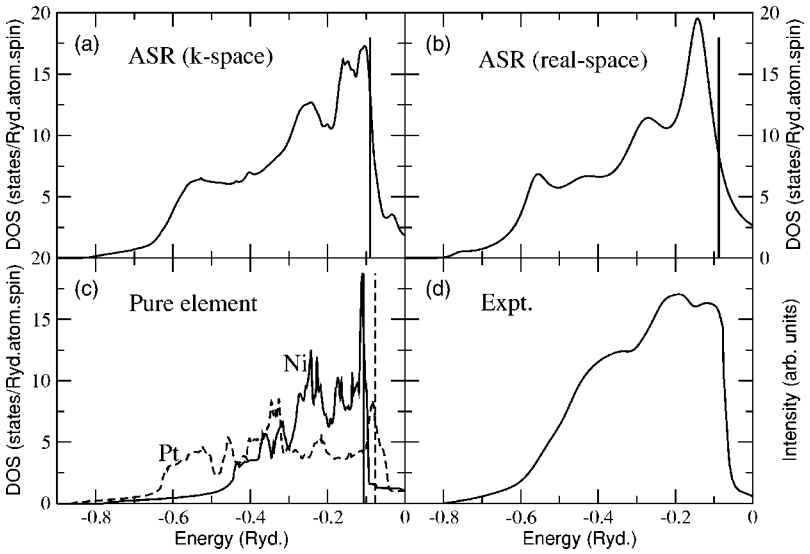

FIG. 6. Comparison of the density of states of the $Ni_{50}Pt_{50}$ alloy calculated using augmented space recursion in (a) **k** space formulation and (b) real space formulation. (c) Density of states of Ni (solid line) and Pt (dotted line) on a lattice appropriate to the $Ni_{50}Pt_{50}$ alloy. (d) Valence-band photoemission spectra of $Ni_{50}Pt_{50}$ with photon energy $h\nu=60$ (Ref. 27).

duced in the **k** space recursion than in real space. The reason for this is the early truncation of recursion in real space and the consequent finite-size effects to which the more localized *d* states are more susceptible.

In Fig. 6 (top row) we show a comparison between the average DOSs calculated by real and reciprocal space recursions. As discussed before, it is the sharp feature straddling the Fermi energy with a major contribution coming from the Ni *d* states that is not well reproduced in the real space technique. In this point our **k** space calculations agree with the KKR CPA results of Staunton *et al.*[26] In the left lower panel of Fig. 6 we show the DOSs for pure Ni and Pt, but in a lattice with the lattice parameter the same as in the alloy. We may compare this with the DOS for the disordered alloy. The rightmost three peaks at −0.25, −0.16, and −0.11 Ry of the disordered DOS are mostly contributed by Ni whereas the left (lower-energy) structures (large shoulder at −0.57 Ry) come mostly from Pt. The sharp peaks in the elemental results are obviously because of the Van Hove singularities of the DOS. The effect of disorder mainly smears out the sharp peaks present in the DOS. The disorder smearing is more pronounced for the *d*-like parts of the band. We remark that there is very little shift in the DOS-related features between the ordered and disordered states.

Finally, in the right lower panel we show the photoemmission spectrum of $Ni_{50}Pt_{50}$ reported by Nahm *et al.*[27] The general features with a double peak straddling the Fermi energy and a lower-energy shoulder are clearly seen. The photoemission spectra are convolutions of the density of states with a weakly energy- and wave-number-dependent transition matrix. This may lead to shifting and smearing of the prominent peak structures. Keeping this in mind, our **k** space recursion results are in good agreement with experiment.

VI. REMARKS AND CONCLUSION

We have presented an augmented space recursion formulation in reciprocal space. We also present a generalization of the tetrahedron method proposed by Jepsen and Andersen[13] for inverting the spectral functions to obtain the density of states. This technique will be useful for carrying out Brilluoin zone integrals for disordered alloys. We have studied both a model alloy and NiPt. The latter was chosen since it has a sharp structure straddling the Fermi energy and therefore is a sensitive test for the accuracy of our technique.

ACKNOWLEDGMENT

One of us (K.K.S.) would like to thank Professor O. K. Andersen, MPI Stuttgart, for kind hospitality and several important discussions during the time this work was developed.

APPENDIX A: THE AUGMENTED SPACE THEOREM

Let $f(n_R)$ be a function of a random variable n_R, whose binary probability density is given by

$$p(n_R) = x\delta(n_R - 1) + y\delta(n_R).$$

We may then write

$$p(n_R) = -\frac{1}{\pi}\lim_{\delta\to 0} \mathrm{Im}\langle\uparrow_R|[(n_R + i\delta)\mathbf{I} - \mathbf{M}_R]^{-1}|\uparrow_R\rangle.$$

Here, the operator $\mathbf{M}_R$ acts on a space spanned by the eigenvectors $|1_R\rangle$ and $|0_R\rangle$ of $\mathbf{M}_R$, corresponding to eigenvalues 1 and 0; $|\uparrow_R\rangle = \sqrt{x}|1_R\rangle + \sqrt{y}|0_R\rangle$ is called the reference state. Its orthogonal counterpart is $|\downarrow_R\rangle = \sqrt{y}|1_R\rangle - \sqrt{x}|0_R\rangle$. The representation of $\mathbf{M}_R$ in this new basis,

$$\mathbf{M}_R = \begin{pmatrix} x & \sqrt{xy} \\ \sqrt{xy} & y \end{pmatrix}.$$

Now,

$$\langle\langle f(n_R)\rangle\rangle = \int_{-\infty}^{\infty} f(n_R)p(n_R)dn_R$$

$$= -\frac{1}{\pi}\,\mathrm{Im}\int_{-\infty}^{\infty} f(n_R)\langle\uparrow_R|(n_R\mathbf{I}-\mathbf{M}_R)^{-1}|\uparrow_R\rangle dn_R$$

$$= -\frac{1}{\pi}\,\mathrm{Im}\sum_{\lambda=0,1}\sum_{\lambda'=0,1} f(n_R)\langle\uparrow_R|\lambda\rangle$$

$$\times\langle\lambda|(n_R\mathbf{I}-\mathbf{M}_R)^{-1}|\lambda'\rangle\langle\lambda'|\uparrow_R\rangle dn_R$$

$$= \sum_{\lambda=0,1}\langle\uparrow_R|\lambda\rangle f(\lambda)\langle\lambda|\uparrow_R\rangle = \langle\uparrow_R|\tilde{\mathbf{f}}|\uparrow_R\rangle. \qquad \text{(A1)}$$

Here $\tilde{\mathbf{f}}$ is an operator built out of $f(n_R)$ by simply replacing the variable n_R by the associated operator $\mathbf{M}_R$. The above expression shows that the average is obtained by taking the matrix element of this operator for the reference state $|\uparrow_R\rangle$. The full augmented space theorem is a generalization of this for functions of many independent random variables $\{n_R\}$.

APPENDIX B: TERMINATORS

The recursive calculation described earlier gives rise to a set of continued fraction coefficients $\{\alpha_n,\beta_n\}$. In any practical calculation we can go only up to a finite number of steps, consistent with our computational process. In case the coefficients converge, i.e., if $|\alpha_n-\alpha|\leqslant\epsilon$, $|\beta_n-\beta|\leqslant\epsilon$ for $n\geqslant N$, we may replace $\{\alpha_n,\beta_n\}$ by $\{\alpha,\beta\}$ for all $n\geqslant N$. In that case the asymptotic part of the continued fraction may be analytically summed to obtain

$$\Gamma(E) = \frac{1}{2}(E-\alpha-\sqrt{(E-\alpha)^2-4\beta^2})$$

which gives a continuous spectrum $\alpha-2\beta\geqslant E\geqslant\alpha+2\beta$. Since the terminator coefficients are related to the band edges and widths, a sensible criterion for the choice of these asymptotic coefficients is necessary, so as not to give rise to spurious structures in our calculations. Beer and Pettifor[22] suggest a sensible criterion: given a finite number of coefficients, we must choose $\{\alpha,\beta\}$ in such a way as to give, for this set of coefficients, the minimum bandwidth consistent with no loss of spectral weight from the band. Let us call these values $\{\alpha_c,\beta_c\}$. This criterion is easily translated into mathematical terms. The δ function that would carry weight out of the band must then be situated exactly at the band edge. We thus demand that the continued fraction diverge simultaneously at both the top and the bottom of the band.

At the band edges, $\Gamma(\alpha\pm2\beta)=\pm\beta$, and so

$$\langle\langle G(\alpha\pm2\beta)\rangle\rangle = \cfrac{\beta_1^2/2}{\pm\beta-\frac{1}{2}(\alpha_1-\alpha)-\cfrac{\beta_2^2/4}{\pm\beta-\frac{1}{2}(\alpha_2-\alpha)-\cfrac{\beta_3^2/4}{\ddots\cfrac{\beta_N^2/2}{\pm\beta-(\alpha_N-\alpha)}}}}.$$

For a given α, the $(N+1)$ eigenvalues of the finite tridiagonal matrix

$$\begin{pmatrix} \frac{1}{2}(\alpha_1-\alpha) & \frac{1}{2}\beta_2 & 0 & \cdots & \cdots & 0 \\ \frac{1}{2}\beta_2 & \frac{1}{2}(\alpha_2-\alpha) & \frac{1}{2}\beta_3 & \ddots & & \vdots \\ 0 & \frac{1}{2}\beta_3 & \ddots & \ddots & \ddots & \vdots \\ \vdots & \ddots & \ddots & \ddots & \ddots & 0 \\ \vdots & & \ddots & \ddots & \ddots & \frac{1}{\sqrt{2}}\beta_N \\ 0 & \cdots & \cdots & 0 & \frac{1}{\sqrt{2}}\beta_N & (\alpha_N-\alpha) \end{pmatrix}$$

are values at which the Green's function diverges. The maximum and minimum of this set of eigenvalues are those values of β that carry weight out of the band. Thus our choice of α is that value for which the maximum eigenvalue is the largest and the minimum the smallest. Since the terminator only involves β^2 we must have

$$\beta_c = \sup_{\{\alpha\}}\beta_{\max}(\alpha_c) = \inf_{\{\alpha\}}|\beta_{\min}(\alpha_c)|.$$

With this choice the terminator $\Gamma(E)$ has all the Herglotz properties required.

*Electronic address: kamal@bose.res.in
†Electronic address: abhijit@bose.res.in
‡Electronic address: O.Jepsen@fkf.mpg.de

[1] T. Saha, I. Dasgupta, and A. Mookerjee, J. Phys.: Condens. Matter **6**, L245 (1994).
[2] T. Saha, I. Dasgupta, and A. Mookerjee, J. Phys.: Condens. Matter **8**, 1979 (1996).
[3] A function of a complex variable $f(z)$ is called Herglotz if all singularities of $f(z)$ lie on the real z axis and $\mathrm{sgn}[\mathrm{Im}\,f(z)] = -\mathrm{sgn}(\mathrm{Im}\,z)$ for all z off the real axis.
[4] A. Mookerjee and R. Prasad, Phys. Rev. B **48**, 17 724 (1993).
[5] I. Dasgupta, T. Saha, and A. Mookerjee, Phys. Rev. B **51**, 3413 (1995).
[6] T. Saha and A. Mookerjee, J. Phys.: Condens. Matter **8**, 2915 (1996).
[7] A. Chakrabarti and A. Mookerjee, J. Phys.: Condens. Matter **14**, 3211 (2002).
[8] R. Haydock, *Solid State Physics* (Academic Press, New York, 1980), Vol. 35.
[9] K. K. Saha and A. Mookerjee, J. Phys.: Condens. Matter **16**, 1409 (2004).
[10] P. Biswas, B. Sanyal, M. Fakhruddin, A. Halder, A. Mookerjee,

and M. Ahmed, J. Phys.: Condens. Matter **7**, 8569 (1995).
[11] P. Biswas, B. Sanyal, A. Mookerjee, A. Huda, N. Chowdhury, M. Ahmed, and A. Halder, Int. J. Mod. Phys. B **11**, 3703 (1997).
[12] K. K. Saha and A. Mookerjee, Phys. Rev. B **70**, 134205 (2004).
[13] O. Jepsen and O. K. Andersen, Solid State Commun. **9**, 1763 (1971).
[14] G. Lehmann and M. Taut, Phys. Status Solidi B **54**, 469 (1972).
[15] Ph. Lambin and J. P. Vigneron, Phys. Rev. B **29**, 3430 (1984).
[16] A. Mookerjee, J. Phys. C **6**, 1340 (1973).
[17] T. Kaplan and L. J. Gray, Phys. Rev. B **15**, 3260 (1977).
[18] S. Ghosh, N. Das, and A. Mookerjee, Int. J. Mod. Phys. B **21**, 723 (1999).
[19] I. Dasgupta, T. Saha, A. Mookerjee, and G. P. Das, J. Phys.: Condens. Matter **9**, 3529 (1997).
[20] O. K. Andersen, Phys. Rev. B **12**, 3060 (1975).
[21] O. K. Andersen and O. Jepsen, Phys. Rev. Lett. **53**, 2571 (1984).
[22] N. Beer and D. G. Pettifor, in *The Electronic Structure of Complex Systems*, edited by P. Phariseau and W. M. Temmerman, NATO Advanced Studies Institute, Series B: Physics (Plenum, New York, 1982), Vol. 113, p. 769.
[23] R. Haydock, Philos. Mag. B **43**, 203 (1981); R. Haydock and R. L. Te, Phys. Rev. B **49**, 10 845 (1994).
[24] R. Haydock, Ph.D. thesis, University of Cambridge, Cambridge, U.K., 1972.
[25] A. H. MacDonald, S. H. Voskot, and P. T. Coleridge, J. Phys. C **12**, 2991 (1979).
[26] F. J. Pinski, B. Ginatempo, D. D. Johnson, J. B. Staunton, G. M. Stocks, and B. L. Gyorffy, Phys. Rev. Lett. **66**, 766 (1991).
[27] T-U. Nahm, J-Y. Kim, S-J. Oh, S-M. Chung, J-H. Park, J. W. Allen, K. Jeong, and S. Kim, Phys. Rev. B **54**, 7807 (1996).